

Adaptive Carrier Smoothing Using Code and Carrier Divergence

Euiho Kim, Todd Walter, and J.D. Powell, *Stanford University*

BIOGRAPHY

Euiho Kim is a Ph.D. candidate in the Aeronautics and Astronautics Department at Stanford University. He received his B.S. in Aerospace Engineering in 2001 from Iowa State University and his M.S. from Stanford University in 2002. His research currently focuses on precise positioning using GPS/WAAS and flight inspection truth systems.

Dr. Todd Walter received his B. S. in physics from Rensselaer Polytechnic Institute and his Ph.D. in 1993 from Stanford University. He is currently a Senior Research Engineer at Stanford University. He is a co-chair of the WAAS Integrity Performance Panel (WIPP) focused on the implementation of WAAS and the development of its later stages. Key contributions include: early prototype development proving the feasibility of WAAS, significant contribution to MOPS design and validation, co-editing of the Institute of Navigation's book of papers about WAAS and its European and Japanese counterparts, and design of ionospheric algorithms for WAAS. He was the co-recipient of the 2001 ION early achievement award.

Prof. J. David Powell received his B.S. degree in Mechanical Engineering from MIT and his Ph.D in Aero/Astro from Stanford in 1970. He joined the Stanford Aero/Astro Department Faculty in 1971 and is currently an Emeritus Professor. Recent focus of research is centered around applications of GPS: applications of the FAA's WAAS for enhanced pilot displays, the use of WAAS and new displays to enable closer spacing on parallel runways, and the use of WAAS for flight inspection for conventional navigation aids. He has co-authored two text books in control systems design.

ABSTRACT

This paper investigates an adaptive carrier smoothing for a single frequency GPS user. Using a Hatch filter in a single frequency receiver reduces multipath and receiver noise but introduces an induced bias that depends on the rate of ionospheric delay and a carrier smoothing time. Ideally, to use a Hatch filter more effectively and efficiently, the rate of ionospheric delay and noise

characteristics should be known. However, since these are usually not known to a single frequency user, a conservative constant carrier smoothing time is typically used for safety of life applications such as WAAS and LAAS.

This paper starts by introducing how to estimate the rate of ionospheric delay with white noise-like multipath and highly correlated multipath from code and carrier divergence (CCD). For the different multipath characteristics, the ordinary least square (OLS) or the (feasible) generalized least square (GLS) estimators is used. Given the estimated ionospheric delay rate, multipath can be separated and is modeled as white noise or a cosine wave according to the multipath characteristics. The estimated rate of ionospheric delay and the modeled multipath are used to construct a cost function. From the cost function, it is possible to compute an optimal carrier smoothing time which balances the reduction of multipath against the magnitude of the induced bias. These processes are repeated every 60 seconds and update the optimal carrier smoothing time by keep observing the ionospheric rate and multipath. Preliminary results show that this technique significantly suppresses multipath and does not introduce any noticeable large drifts.

INTRODUCTION

The carrier-smoothing (Hatch) filter has been widely used in GPS community. The filter smoothes noisy pseudo range measurements by using precise but ambiguous carrier phase measurements. However, this filter introduces a bias in the filtered range due to the divergence of code and carrier measurements. The magnitude of the bias is a function of a carrier smoothing time and ionospheric delay gradients. When a user increases the smoothing time, the user obtains smoother measurements but suffers a bigger bias due to the ionospheric delay gradients. Therefore, there is a trade-off between smoothness and an induced bias in using a Hatch filter.

Typically, a carrier smoothing time is preset based on a user's requirement and kept constant during operation. The requirements are compromised from the induced bias

and the smoothness of the filtered ranges. To high integrity users, these preset smoothing times are chosen by considering worst conditions in terms of ionospheric delay gradients and noise in the code phase measurements, which may not fully take advantage of a Hatch filter. To avoid the disadvantage for a single frequency user, various methods have been proposed to mitigate multipath: a kalman filter with a modeled platform dynamics [1], a complementary kalman filter with GPS velocity [2], and an optimal hatch filter using a multipath model parameterized by an elevation angle and Klobuchar model [3].

This paper introduces a method how a single frequency receiver user can select the optimal carrier smoothing time. Unlike the previous approaches, this method directly estimates time-varying slant ionospheric delay rates and multipath in code phase measurements. Using these estimates, two cost functions are constructed for white noise multipath and highly correlated multipath to give an optimal carrier smoothing time that minimizes the cost functions to balance an induced bias and multipath effect. This optimal carrier smoothing time is used in a Hatch filter, and this whole procedure is repeated at a certain rates.

This paper is structured as follows. First, linear regression theory is briefly reviewed because it is extensively used to estimate time-varying slant ionospheric delay gradients. Second, estimation scheme of the slant ionospheric delay rates and multipath characteristics using code minus carrier phase measurements will be discussed. Third, given estimated ionospheric delay rate and multipath, the formulation of cost functions with respect to white noise multipath and highly correlated multipath will be discussed. Fourth, tests of real data will be shown and discussed. Lastly, discussion and conclusion will be followed.

OVERVIEW OF LINEAR REGRESSION

A. Simple Linear Regression with White Noise

When the relationship between an observation, y , and a regressor, x , is linear, y can be modeled as [4]

$$y = \beta_0 + \beta_1 x + \varepsilon \quad (1)$$

where β_0 is the intercept, β_1 is the slope, and $\varepsilon \sim \text{WN}(0, \sigma^2)$ is white noise.

When the time series of the observation, y , are available, the linear model can be described in a matrix form as

$$Y = X\beta + \varepsilon \quad (2)$$

where Y is a $n \times 1$ vector, X is a $n \times 2$ matrix, β is a 2×1 vector, and ε is a $n \times 1$ vector.

If we can assume that the linear model is correct, the unbiased and the most efficient estimate of β can be obtained from the ordinary least-squares (OLS) which is

$$\hat{\beta}_{OLS} = (X^T X)^{-1} X^T Y \quad (3)$$

The variance of $\hat{\beta}_{OLS}$ is

$$\text{Var}(\hat{\beta}_{OLS}) = \sigma^2 (X^T X)^{-1} \quad (4)$$

B. Linear Regression with Autocorrelated Noise

When the noise is autocorrelated, the ordinary least-squares still gives an unbiased solution, but the variance is no longer minimized. In this case, the generalized least-squares gives the best solution.

The linear model with autocorrelated noise is

$$\begin{aligned} Y &= X\beta + \varepsilon \\ E(\varepsilon) &= 0, \text{Var}(\varepsilon) = \sigma^2 V \end{aligned} \quad (5)$$

where V is a nonsingular and positive definite matrix.

The unbiased and the most efficient solution for equation (5) is

$$\hat{\beta}_{GLS} = (X^T V^{-1} X)^{-1} X^T V^{-1} Y \quad (6)$$

The variance is

$$\text{Var}(\hat{\beta}_{GLS}) = \sigma^2 (X^T V^{-1} X)^{-1} \quad (7)$$

The generalized least-squares (GLS) requires a covariance matrix, V , of the noise to estimate the coefficients β . However, the covariance matrix is usually unknown either. Therefore, it is necessary to estimate the covariance matrix and the coefficients at the same time. This is well-known problem in econometrics and can be solved by using a 2 step process, also called as a feasible generalized least-squares (FGLS) [5].

The FGLS algorithm is

find β_{OLS} from OLS and compute residuals

$$e = Y - X\beta_{OLS}$$

1) *Fit an ARMA model to e*

- 2) Find β_{GLS} using V computed from the ARMA model
- 3) Compute $e = Y - X\beta_{GLS}$
- 4) Return to 1) until β_{GLS} stabilizes

The FGLS includes AutoRegressive-Moving Average (ARMA) modeling to the residual errors. Discussion about ARMA modeling can be also found in [5].

ESTIMATION OF SLANT IONOSPHERIC DELAY RATES AND MULTIPATH IN CODE PHASE MEASUREMENTS USING LINEAR REGRESSION

A. Linear Model for Code minus Carrier Phase Measurements

The basic measurements in a GPS receiver are code and carrier phase measurements. The code phase measurements, ρ , and the carrier phase measurements, Φ , can be written as

$$\begin{aligned}\rho &= r + c[\delta t_u - \delta t_s] + I + T + M_\rho \\ \Phi &= r + c[\delta t_u - \delta t_s] - I + T + N + M_\Phi\end{aligned}\quad (8)$$

where r is the true range between a receiver and a satellite. c is the speed of light. δt_u and δt_s are receiver and satellite clock errors, respectively. I is ionospheric delay and T is tropospheric delay. N is an integer ambiguity. M_ρ and M_Φ include multipath, thermal noises, and modeling errors in the code and carrier phase measurements respectively. Since multipath is usually bigger than other receiver related noise, M_ρ and M_Φ will be considered as multipath in code and carrier phase measurements.

The difference, y , between ρ and Φ at time t is

$$\begin{aligned}y_t &= \rho_t - \Phi_t \\ &= 2I_t - N + M_{t,\rho} - M_{t,\Phi}\end{aligned}\quad (9)$$

This difference includes ionospheric delays multiplied by 2, a bias, and multipath. Our interest here is to estimate slant ionospheric delay rates and separate the multipath from the other terms. Before jumping into this problem, it should be noted that the ionospheric delays slowly change with respect to time during nominal ionospheric days. Therefore, the rate can be seen as a constant during a short time window (tens of minutes). Then, equation (9) can be rewritten as

$$\begin{aligned}y_t &= \beta_0 + 2t \cdot \beta_1 + M_{t,\rho} - M_{t,\Phi} \\ &\approx \beta_0 + 2t \cdot \beta_1 + M_{t,\rho}\end{aligned}\quad (10)$$

In equation (10), $M_{t,\Phi}$ is ignored because it is much smaller than $M_{t,\rho}$.

Expressing the time series of equation (10) in a matrix form yields

$$\begin{aligned}\begin{bmatrix} y_{t_1} \\ y_{t_2} \\ \vdots \\ y_{t_n} \end{bmatrix} &= \begin{bmatrix} 1 & 2 \cdot t_1 \\ 1 & 2 \cdot t_2 \\ \vdots & \vdots \\ 1 & 2 \cdot t_n \end{bmatrix} \begin{bmatrix} \beta_0 \\ \beta_1 \end{bmatrix} + \begin{bmatrix} M_{t_1,\rho} \\ M_{t_2,\rho} \\ \vdots \\ M_{t_n,\rho} \end{bmatrix} \\ Y &= X\beta + M\end{aligned}\quad (11)$$

Now, the problem becomes to find β in the presence of M . If M is close to white noise, the ordinary least-squares (OLS) is the best estimator. However, if M is highly correlated, the feasible generalized least-squares (FGLS) should be used instead of the OLS.

B. Multipath Estimation and Its Characteristics from Dynamic and Static GPS Receiver Measurements

In general, the multipath characteristics are closely related to the motion of the platform where a GPS antenna is installed. Airborne and static ground measurements are considered in this section because they have white noise multipath and highly correlated multipath.

Assuming that we have a good estimate of $\hat{\beta}$, the estimated multipath can be separated as followings.

$$\hat{M} = Y - X\hat{\beta}\quad (12)$$

Figure 1 shows a time series of mean subtracted airborne code minus carrier phase measurements and its fitted line using first order linear regression.

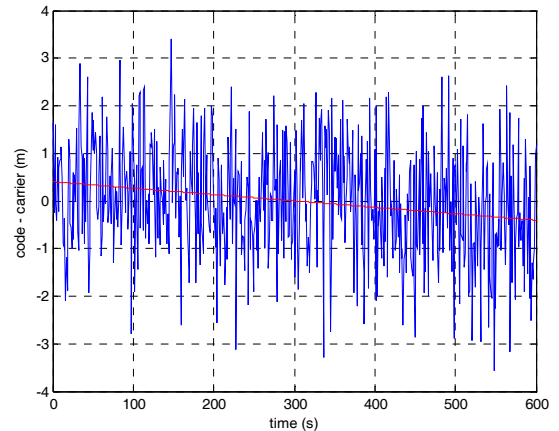


Figure 1: Mean subtracted code minus carrier over 600s

with a regressed line for airborne measurements

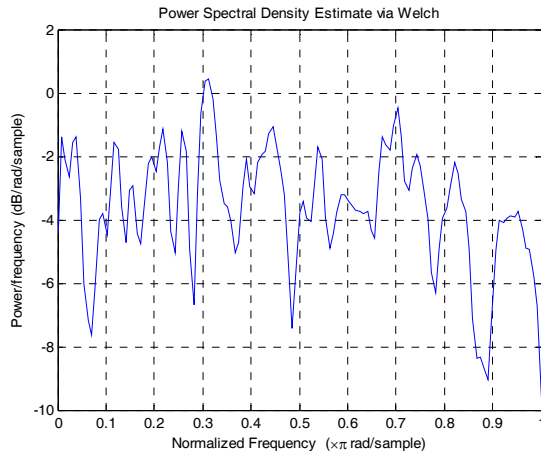


Figure 2: Power spectral density of airborne multipath in code minus carrier phase measurements

The power spectral density of the residuals in figure 1 is shown in figure 2 which indicates that the multipath can be approximated as white noise. Therefore, it should be reasonable to use the OLS to estimate the ionospheric delay gradients.

Figure 3 shows a time series of mean subtracted static ground code minus carrier phase measurements and its fitted line using first order linear regression.

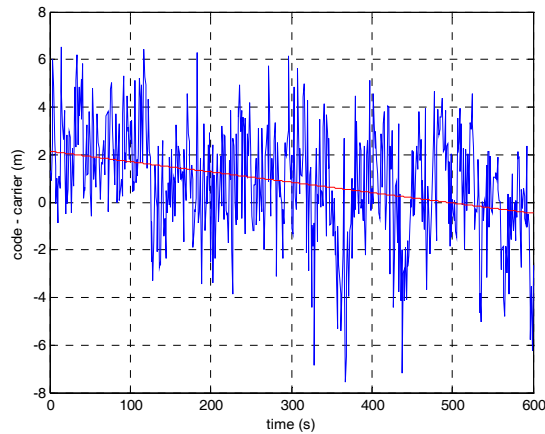


Figure 3: Mean subtracted code minus carrier over 600s with a regressed line for static ground measurements

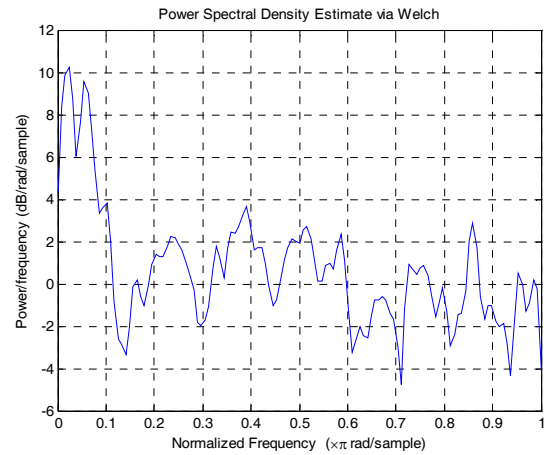


Figure 4: Power spectral density of static ground noise in code minus carrier measurements

Figure 4 shows the power spectral density of the residuals in figure 3. It shows that the residuals have a significant low frequency noise, from which we can conclude that the noise is highly autocorrelated. Therefore, the FGLS is desirable for this case.

In this subsection, it is shown that the OLS is appropriate to be used in airborne measurements and the FGLS in static ground measurements. However, the OLS is much easier to be implemented and preferable in practice than the FGLS. In the next subsection, the feasibility of using the OLS on the measurements with correlated noise will be discussed.

C. Comparison of the Estimated Slant Ionospheric Delay Rates Using the OLS and the FGLS on the Measurements with Autocorrelated Noise

The feasible generalized least squares (FGLS) is an asymptotically optimal estimator when noise is correlated. Even though it is desirable to use the FGLS, the FGLS is quite computationally intensive to be used in real time. Therefore, we should make sure that it is worth while to pursuit the FGLS with the burden of the heavy computation for our applications.

The FGLS and the OLS are implemented on the 800 seconds window of static ground measurements whose multipath has a strong correlation, and figure 5 shows that the difference of the results from the FGLS and the OLS.

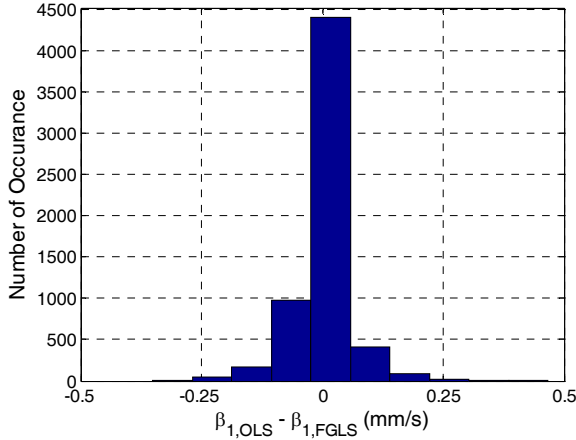


Figure 5: Histogram of the difference of the estimated ionospheric delay rates from using the OLS and the FGLS

The mean of the difference in the histogram is -0.0004 mm/s mean, and the standard deviation is 0.06 mm/s. These statistics are insignificant for most of applications since slant ionospheric delay rates of tens of mm/s are of a concern in practice. Thus the OLS can be used instead of the FGLS on the code minus carrier phase measurements having autocorrelated noise.

D. Evaluation of the Estimated Slant Ionospheric Delay Rates with Dual Frequency Measurements

In the previous subsection, it is shown that the OLS can be used instead of the FGLS without much sacrifice. Therefore, the estimated ionospheric delay rates from the OLS are used. In order to check adequacy of our model, measurements from a dual frequency receiver are used.

The reference ionospheric delay rates from a dual frequency receiver are computed as follows [6].

$$S_{L1,t} = \frac{f_{L2}^2}{f_{L1}^2 - f_{L2}^2} [(\Phi_{L1} - N_{L1}) - (\Phi_{L2} - N_{L2})]_t \quad (13)$$

$$\Delta I_{t,dual} = S_{L1,t} - S_{L1,t-1}$$

where f_{L1} and f_{L2} are the center frequencies of $L1$ and $L2$ bands. It should be noted that $\Delta I_{t,dual}$ from a dual frequency receiver is a direct estimate of an ionospheric delay and include some noise.

Figure 6 shows $\Delta I_{t,dual}$ and $\hat{\beta}_{t,1}$ for one satellite computed from implementing the OLS on static ground measurements on a nominal ionospheric day. These estimates are computed at every 15 seconds and a 800 seconds sliding window is used to estimate $\hat{\beta}_{t,1}$. Since raw $\Delta I_{t,dual}$ is quite noisy, it is smoothed by a non-causal moving average filter and shown as a green line in the

plot. The $\hat{\beta}_{t,1}$ is also filtered by using a causal moving average filter because estimates using window are also likely to have some noise. Unlike $\Delta I_{t,dual}$, $\hat{\beta}_{t,1}$ is filtered because smoothing is impossible in real time. The smoothing and filtering process uses past 30 minutes of estimates. From figure 6, we can see that the filtered slant ionospheric delay rate, shown as a red line, using the linear model closely follows the measured slant ionospheric delay rates from a dual frequency receiver.

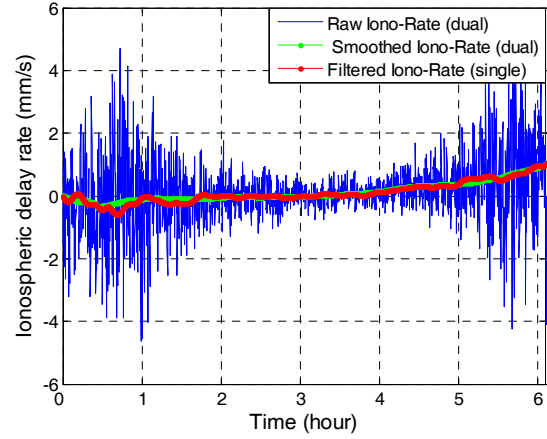


Figure 6: Comparison of the estimated ionospheric delay rates from a dual frequency receiver and from using the linear model during

Figure 7 shows the histogram of the difference between $\Delta I_{t,dual}$ and $\hat{\beta}_{t,1}$ for all satellites in view during 19 hours on Oct 26, 2006 at Atlantic City. The mean of the difference is -0.047 mm/s, and the standard deviation is 0.15 mm/s. These results indicate that the linear model is quite satisfactory for many applications.

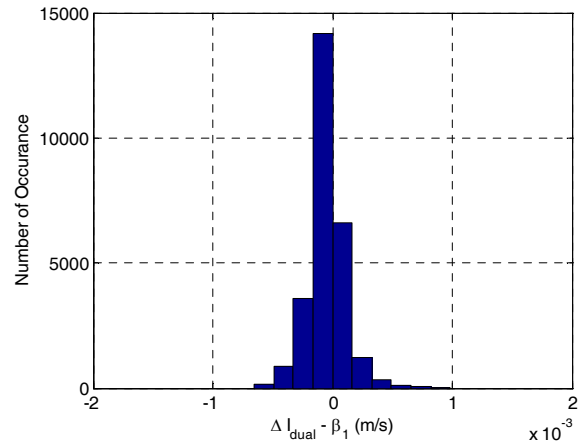


Figure 7: Histogram of the difference between smoothed $\Delta I_{t,dual}$ and $\hat{\beta}_{t,1}$ for all in view during 19 hours on Oct 26, 2006 at Atlantic City

OPTIMAL CARRIER SMOOTHING BASED ON THE ESTIMATES OF SLANT IONOSPHERIC DELAY RATES AND MULTIPATH

Errors in smoothed range using a Hatch filter need to be identified to formulate a cost function. An optimal carrier smoothing is naturally the one that minimizes the cost function. This section shows the errors in carrier smoothed range and derivation of two cost functions that differs with respect to multipath characteristics.

A. Errors in Carrier Smoothed Range

Using a Hatch filter, the carrier-smoothed pseudorange at time t , $\bar{\rho}_t$, is given by

$$\bar{\rho}_t = \frac{1}{k} \rho_t + \frac{k-1}{k} (\bar{\rho}_{t-1} + \Phi_t - \Phi_{t-1}) \quad (14)$$

where ρ is a code phase measurement, Φ_t is a carrier phase measurement, and k is a carrier smoothing time.

We can define the error, ε , in the smoothed pseudorange as [7]

$$\varepsilon_t = \bar{\rho}_t - r_t - c[\delta t_u - \delta t_s] - T_t - I_t \quad (15)$$

This error has the following dynamics.

$$\varepsilon_t = \frac{k-1}{k} \varepsilon_{t-1} - 2 \frac{k-1}{k} (I_t - I_{t-1}) + \frac{1}{k} M_t \quad (16)$$

If we consider the initial error, ε_0 , to zero and a constant ionospheric delay rate such as $(I_t - I_{t-1}) = a$, then the solution of the error is given by

$$\varepsilon_t = -2 \sum_{i=0}^{t-1} \phi^{i+1} a + \frac{1}{k} \sum_{i=0}^{t-1} \phi^i M_{t-i} \quad (17)$$

where $\phi = \frac{k-1}{k}$. The assumption on the constant ionospheric delay rate is valid for tens of minutes in nominal ionospheric days.

Furthermore, when t is large, the steady state error, ε_{ss} , becomes

$$\begin{aligned} \varepsilon_{ss} &= -2 \left(\frac{\phi}{1-\phi} \right) a + \frac{1}{k} \sum_{i=0}^{t-1} \phi^i M_{t-i} \\ &= -2(k-1)a + \frac{1}{k} \sum_{i=0}^{t-1} \phi^i M_{t-i} \end{aligned} \quad (18)$$

From equation (18), it should be noted that the steady state error, ε_{ss} , of the carrier smoothing filter is a function of the rate of ionospheric delays, multipath in the code phase measurements, and a carrier smoothing time. Equation (18) says that the larger a carrier smoothing time is, there are a bigger induced bias and lesser effects of multipath in ε_{ss} .

B. Cost Function with White Noise Multipath

The error contributed from white noise multipath in equation (18) is

$$\varepsilon_{Mw} = \frac{1}{k} \sum_{i=0}^{t-1} \phi^i M_{t-i} \quad (19)$$

When the multipath is assumed to be white, i.e

$\{M_n\} \sim WN(0, \sigma^2)$, the variance of ε_{Mw} can be computed as follows.

$$\begin{aligned} E(\varepsilon_{Mw})^2 &= E\left(\frac{1}{k} \sum_{i=0}^{t-1} \phi^i M_{t-i}\right)^2 \\ &= \frac{1}{k^2} E\left(\sum_{i=0}^{t-1} \phi^i M_{t-i} \sum_{j=0}^{t-1} \phi^j M_{t-j}\right) \\ &= \frac{1}{k^2} E\left(\sum_{i=0}^{t-1} \phi^{2i} M_{t-i}^2\right) \\ &= \frac{\sigma^2}{k^2} \left(\frac{1}{1-\phi^2}\right) \\ &= \frac{\sigma^2}{k^2} \left(\frac{1}{1-\left(\frac{k-1}{k}\right)^2}\right) \\ &= \frac{\sigma^2}{2k-1} \end{aligned} \quad (20)$$

Therefore, a cost function for white noise multipath can be defined as follows.

$$\begin{aligned} J_w(k) &= \mu J_I + J_{Mw} \\ &= 4\mu(k-1)^2 a^2 + \frac{\sigma^2}{2k-1} \end{aligned} \quad (21)$$

where a and σ are assumed to be given. μ is a weighting factor. J_I is the square of the induced bias and J_{Mw} is the variance of filtered multipath.

Figure 8 shows optimal k 's chosen with respect to given ionospheric rates and standard deviations of multipath when μ is set to 0.05.

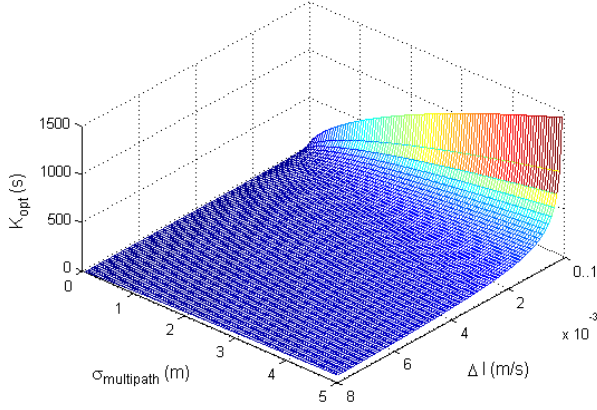


Figure 8: Optimal k 's with white noise multipath assumption

Figure 9 and 10 shows the expected induced bias and variance of filtered multipath when using the optimal k in figure 8. The induced bias and the variance are the decision criteria that a user bases on to choose μ and an optimal k .

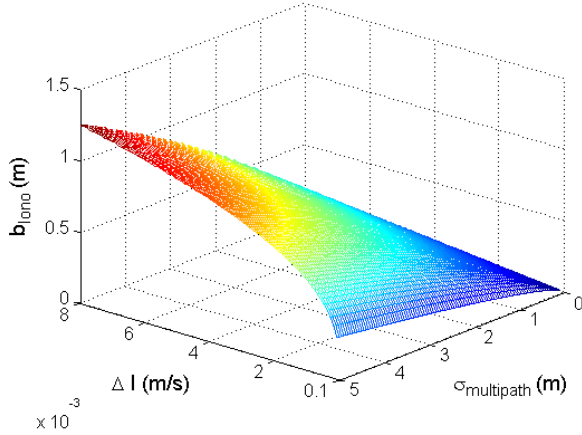


Figure 9: Induced bias from using optimal k 's from figure 8.

The assumption on the white noise multipath is not valid to static ground users but is reasonable to airborne as shown in a previous section. Therefore, the optimal k obtained from white noise multipath is recommended to airborne users.

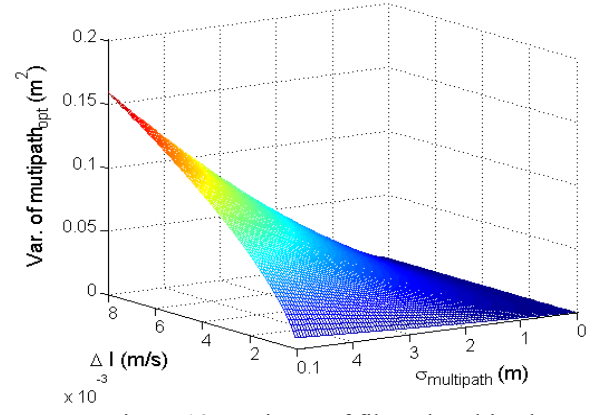


Figure 10: Variance of filtered multipath from using optimal k 's from figure 8

C. Cost Function with Sinusoidal Multipath

The highly correlated multipath on ground can be seen as a quasi-sinusoidal wave. This quasi-sinusoidal wave also can be seen as the weighted sum of infinitely many sine and cosine waves. Among the many waves, a low frequency noise is difficult to be filtered in general. Also, this is the case in using a Hatch filter, which gives hints of how to treat the quasi-sinusoidal wave in the formulation of the cost function.

Let us model quasi-sinusoidal multipath as a cosine wave

$$M_s = A \cos(\omega \cdot t + \alpha) \quad (22)$$

where A is an amplitude, ω is the distinct low frequency that has high power and α is an unknown phase. A reasonable guideline to determine A and ω is as follows.

- 1) Compute Fast Fourier Transform (FFT) of multipath
- 2) Find the frequency which has the most distinct magnitude in low frequency, and designate it as ω
- 3) Compute the sampled σ and designate A as 2σ

Figure 11 shows true multipath and a modeled cosine wave. The true multipath is separated from code minus carrier phase measurements measured from a static ground antenna using the OLS. Therefore, the separated multipath has the characteristics of ground multipath.

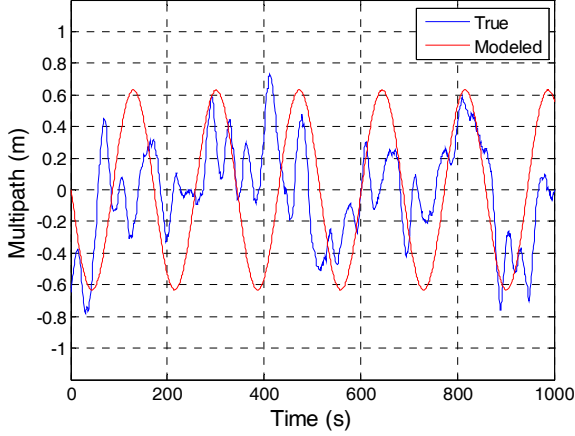


Figure 11: True multipath and a modeled sine wave

When the modeled cosine wave is put into a Hatch filter, the output, ε_{Ms} , has the following expression with a large t .

$$\begin{aligned}
 \varepsilon_{Ms} &= \frac{A}{k} \sum_{i=0}^{t-1} \phi^i \cos(\omega i + \alpha) \\
 &= \frac{A}{k} \sum_{i=0}^{t-1} \frac{\phi^i}{2} (e^{j(\omega i + \alpha)} + e^{-j(\omega i + \alpha)}) \\
 &= \frac{A}{2k} \sum_{i=0}^{t-1} [(\phi e^{j\omega})^i e^{j\alpha} + (\phi e^{-j\omega})^i e^{-j\alpha}] \\
 &= \frac{A}{2k} \left[\frac{e^{j\alpha}}{1 - \phi e^{j\omega}} + \frac{e^{-j\alpha}}{1 - \phi e^{-j\omega}} \right] \\
 &= \frac{A}{2k} \frac{e^{j\alpha} + e^{-j\alpha} - \phi(e^{j(\omega - \alpha)} + e^{-j(\omega - \alpha)})}{1 - \phi e^{j\omega} - \phi e^{-j\omega} + \phi^2} \\
 &= \frac{A \cos(\alpha) - \phi \cos(\alpha - \omega)}{k (1 - 2\phi \cos(\omega) + \phi^2)} \\
 &= \frac{A \cos(\alpha - \omega)}{k \sqrt{1 - 2\phi \cos(\omega) + \phi^2}}
 \end{aligned} \tag{23}$$

Then, the amplitude of the filtered cosine wave, A_F , is

$$A_F = \frac{A}{k \sqrt{1 - 2\phi \cos(\omega) + \phi^2}} \tag{24}$$

Figure 12 shows the outputs of the true and the modeled multipath from a Hatch filter when $k=100$. In this simulation, an ionospheric delay rate is set to 0. The bound of the filtered cosine wave in steady state is $\pm A_F$. From this figure, we can see that this bound very closely indicates the maximum and the minimum values of the filtered true multipath.

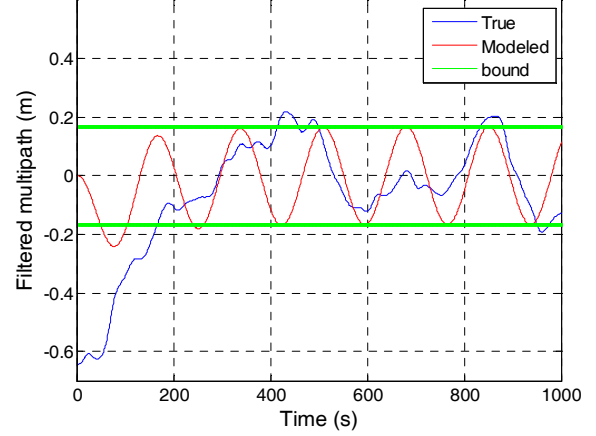


Figure 12: Filtered multipath of the true and the modeled multipath from a Hatch filter.

Then, a cost function with a sinusoidal multipath, J_s , can be constructed as the sum of the cost due to an induced bias and the cost due to A_F .

$$\begin{aligned}
 J_s &= \mu J_I + J_{Ms} \\
 &= 4\mu(k-1)^2 a^2 + \frac{A^2}{k^2 (1 - 2\phi \cos(\omega) + \phi^2)}
 \end{aligned} \tag{25}$$

Figure 13 shows optimal k 's chosen with respect to given ionospheric gradients and amplitudes. μ is set to 1 and ω is set to 0.04 rad/s which has 157 seconds period and is commonly observed from static ground measurements.

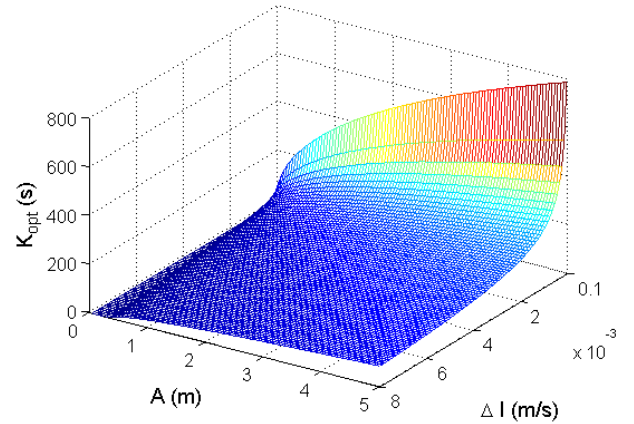


Figure 13: Optimal k 's with sinusoidal multipath assumption

Figure 14 and 15 shows the induced bias and the amplitude of a filtered cosine wave when using optimal k 's in figure 13.

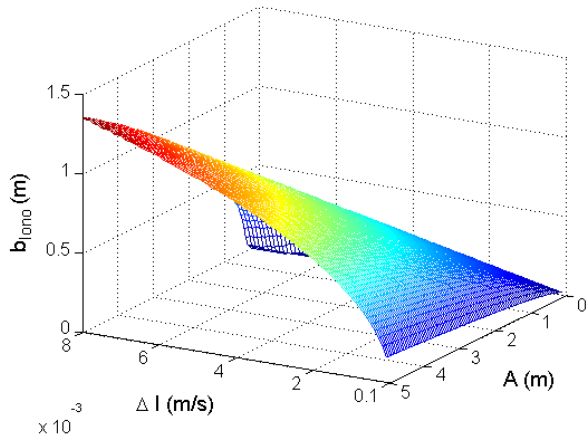


Figure 14: Induced bias from using optimal k 's from figure 13.

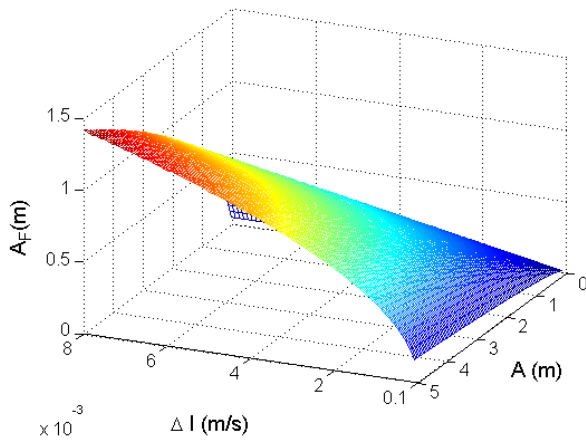


Figure 15: Amplitudes of a filtered cosine wave with $\omega = 0.04$ rad/s from using optimal k 's from figure 13.

ADAPTIVE CARRIER SMOOTHING PROCEDURES

As a summary for the previous long discussion, the adaptive carrier smoothing procedures are illustrated in figure 16.

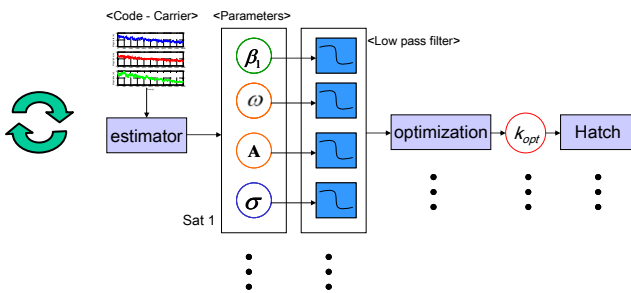


Figure 16: Adaptive carrier smoothing procedures

At first, the estimator takes code minus carrier phase measurements for all satellites and outputs estimated parameters: slant ionospheric delay rates and standard deviation of multipath for white noise multipath assumption and ionospheric delay rates, amplitude and distinct low frequency for the modeled cosine wave for highly correlated multipath assumption. These estimates are low pass filtered, and the optimizer selects an optimal carrier smoothing time from the cost functions. Then, the optimal smoothing time is put into a Hatch filter. These procedures are repeated at a certain rate to adapt to the change of circumstances.

RESULTS

The adaptive carrier smoothing techniques are implemented on airborne measurements and static ground measurements. The sliding window of code minus carrier phase measurements is set to 800 seconds. The parameters are estimated every 15 seconds and filtered using a low pass filter. Therefore, the optimal carrier smoothing time is also updated every 15 seconds. The results are presented in this section with respect to airborne measurements and static ground measurements.

A. Airborne Measurements

Figure 17 shows estimated standard deviation of multipath, $\hat{\sigma}_{multipath}$, and estimated slant ionospheric delay rates over time, \hat{a} , for one satellite. Figure 18 shows optimal k corresponding to the estimated parameters in figure 17.

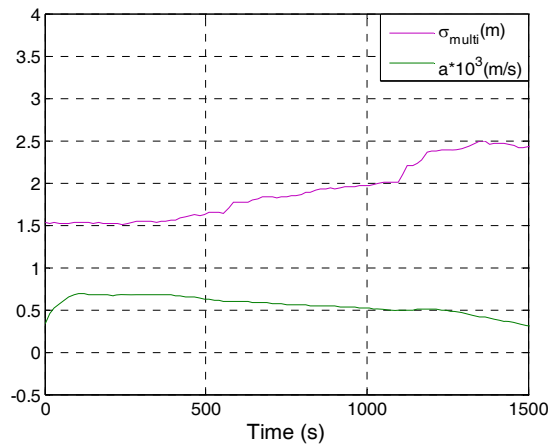


Figure 17: $\hat{\sigma}_{multipath}$ and \hat{a} over time for one satellite

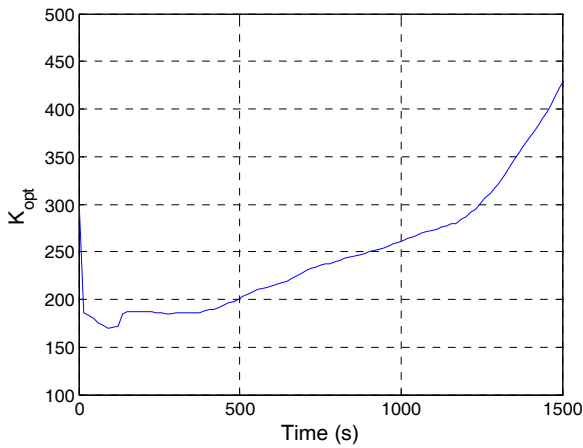


Figure 18: Optimal k corresponding to The estimated parameters in figure 17

In figure 17, $\hat{\sigma}_{multipath}$ increases over time, but \hat{a} decreases. Therefore, optimal k is increasing because a user will have smoother position solutions without adding a significant induced bias to them.

Figure 19 compares position solutions obtained from using a 100 seconds Hatch filter and the adaptive carrier smoothing with white noise multipath assumption. Interestingly, significant noise reduction is observed during 1700~2200 seconds from using the adaptive carrier smoothing than the other times. The reason is that there were two satellites at very low elevation angles, and severe multipath was observed in the code phase measurements. Figure 20 shows the elevations angles over time of all satellites used in the test.

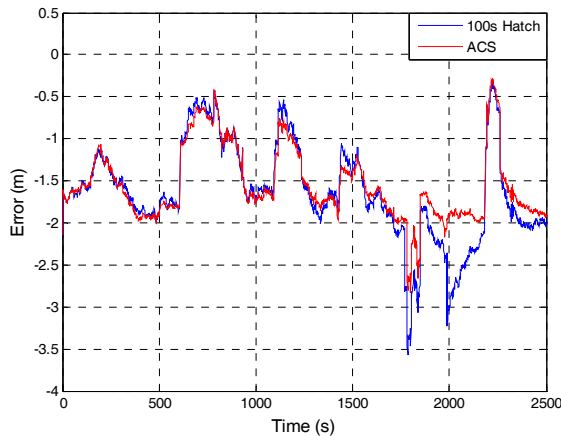


Figure 19: Difference of position solutions using an 100s hatch filter and the adaptive carrier smoothing with white noise multipath assumption

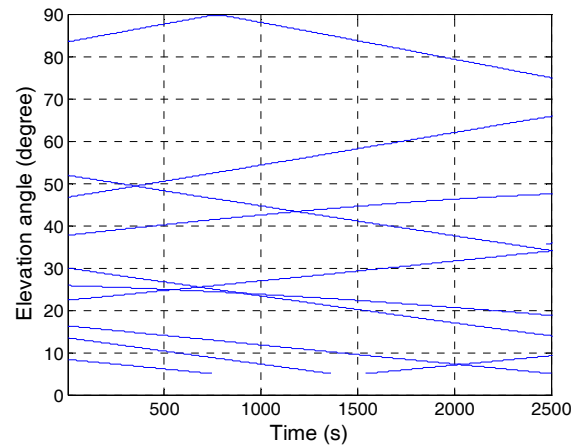


Figure 20: The elevation angles in degrees of the satellites in the test for airborne measurements.

B. Static Ground Measurements

Figure 21 shows the amplitude and frequency for the cosine wave, \hat{A}_F and $\hat{\omega}$, and estimated slant ionospheric delay rate, \hat{a} , for one satellite.

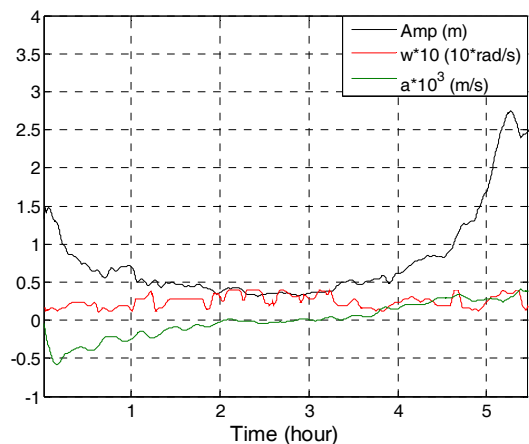


Figure 21: Optimal k over time with respect to \hat{A}_F , $\hat{\omega}$, and \hat{a}

Figure 22 shows the behavior of the optimal k corresponding to the estimated parameters in figure 19. There are several large peaks of the smoothing time when the ionospheric delay rate is very close to zero. In principle, the smoothing time can increase up to infinity when the ionospheric delay rate is exactly zero.

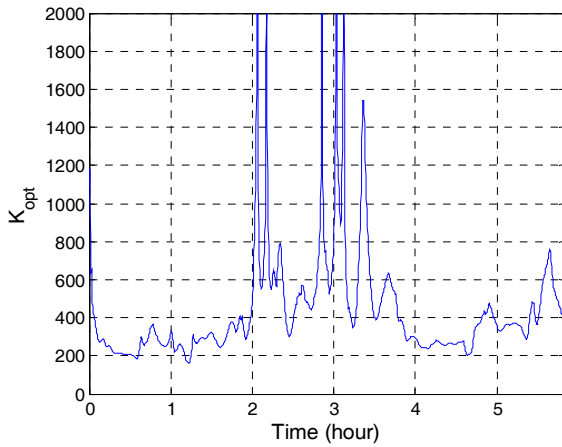


Figure 22: Optimal k corresponding to the estimated parameters in figure 19

Figure 23 compares position solutions obtained from using a 100 seconds Hatch filter and the adaptive carrier smoothing with sinusoidal multipath assumption. In this example, ionospheric delay gradients are small for all satellites, thus the adaptive carrier smoothing gives much smoother position solutions. The difference of the two position solutions are more clearly shown in figure 23 than figure 19.

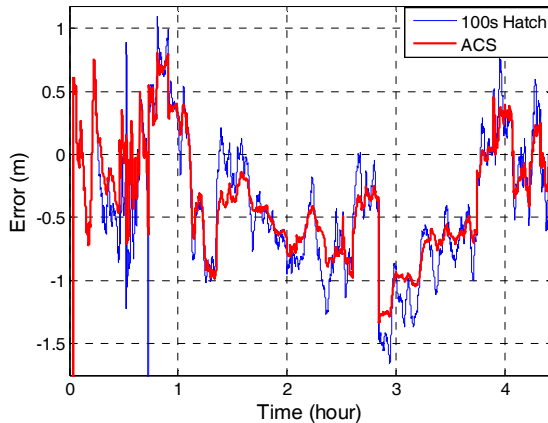


Figure 23: Difference of position solutions using an 100s hatch filter and the adaptive carrier smoothing with sinusoidal multipath assumption

DISCUSSION

It is shown that the estimation of slant ionospheric delay rates with a single frequency receiver is very promising. It is observed that the estimates are exceptionally good when a satellite is at high elevation angles. But, when an elevation angle is low, the estimates have errors as much as 1mm/s. The reasons for the relatively poorer performance at low elevation angles are severe multipath and a rapid change of variance of multipath. The problem due to change of the variance can be fixed by using variance-stabilizing transformations [4], but the severe

multipath at low elevation angles will still make it difficult to estimate accurate slant ionospheric delay rates. Therefore, when satellites are at low elevation angles, high integrity users are recommended to limit a maximum carrier smoothing time or compute an optimal carrier smoothing time by setting a minimum ionospheric delay rates based on a confidence interval. For white noise multipath, the 95% confidence interval for the ionospheric delay rate is $\hat{\beta}_{i,1} \pm 0.6$ mm/s when a 800s sliding window and a standard deviation of 2m are considered.

CONCLUSION

Throughout this paper, the adaptive carrier smoothing technique is introduced for white noise multipath and highly correlated multipath. This technique is tested both on dynamic airborne and static ground measurements taken on nominal ionospheric days. From the suggested cost functions and the particular measurements, the optimal carrier smoothing times are usually much bigger than 100 seconds for both airborne and static ground measurements. Since there is no large ionospheric gradient observed, the position solutions using adaptive carrier smoothing are smoother than the position solutions using 100s carrier smoothing time without having a significant induced bias for the both tests.

Even though it is rather hard to quantify the smoothness obtained from using the adaptive carrier smoothing, the difference of the two position solutions can provide rough estimates. For example, in the result for the static ground measurements, the positions using adaptive carrier smoothing tends to be inside the position using 100s Hatch filter. The difference of the two position solutions has a mean close to zero and standard deviations of 22cm in East, 35cm in North, and 56cm in Up. Therefore, roughly speaking, these are the smoothness benefited from using the adaptive carrier smoothing.

Overall, the adaptive carrier smoothing introduced in this paper is expected to be more useful in times or places that ionosphere is very active and multipath is severe. In addition, more aggressive users are recommended to tweak the cost function on their own preferences to better meet their applications.

ACKNOWLEDGMENT

The authors gratefully acknowledge the support of FAA flight inspection division (AVN)

REFERENCES

- [1] P.Y.C. Hwang and R.G. Brown, "Combining Pseudorange with Continuous Carrier Phase Using a Kalman Filter", NAVIGATION, Journal of The Institute of Navigation, Vol. 37, No 2, Summer, 1990
- [2] L. Helena, S. Jari, and T. Jarmo, "Complementary Kalman Filter for Smoothing GPS Position with GPS Velocity", ION GPS/GNSS, 2003, Portland, OR
- [3] B. Park and C. Kee, "Optimal Hatch Filter With a Flexible Smoothing Window Width", ION GNSS 18th International Technical Meeting of the Satellite Division, Sept. 2005, Long Beach, CA
- [4] D.C. Montgomery, E.A. Peck, and G.G. Vining, "Introduction to Linear Regression Analysis", Fourth Edition, Wiley, 2006
- [5] P.J. Brockwell, and R.A. Davis, "Introduction to Time Series and Forecasting", second edition, Springer, 2002
- [6] P. Mirsa and P. Enge, "Global Positioning System", Second edition, Ganga-Jamuna Press, 2006
- [7] T. Walter et al., "The Effects of Large Ionospheric Gradients on Single Frequency Airborne Smoothing Filters for WAAS and LAAS", ION NTM, 2004, San Diego, CA